Journal of Orthopaedic Surgery and Research

RESEARCH

Open Access

Classification in 157 patients with Lisfranc injuries using three-dimensional fracture lines and heat map

Lei Zhang[1,2,3†], Songtao Jiang[4†], Ruihan Wang[5,6†], Xi Cheng[4], Wangyu Wu[7] and Guoyou Wang[1,2,3*]

Abstract

Background Recently Lisfranc fractures have increased due to increased high-energy injuries from various causes. However, due to incomplete traditional classification, the pattern and distribution of fractures cannot be analyzed in three dimensions. This study examines a novel fracture pattern based on the fracture line and heat map for Lisfranc injuries.

Methods We retrospectively analyzed data from CT scans of 157 patients diagnosed with Lisfranc injuries. We extracted the CT data of a healthy adult and created a standard foot model. We performed 3D reconstruction using patients' CT images and superimposed the fracture model onto the standard model for drawing fracture lines. Subsequently, we converted the fracture lines into a heat map for visualization.

Results The novel classification identifies high-density fracture sites within the tarsometatarsal joint, predominantly localized in the medial and lateral columns. The fracture lines not involving the TMT joint are mainly located in the medial aspect of the first metatarsal trunk and the fifth metatarsal trunk. Additionally, we develop an assessment protocol for Lisfranc injury that incorporates ligament injury, displacement, and fracture.

Conclusion The new classification accurately identifies the different types of fractures in Lisfranc injuries, enabling clinicians to more fully and accurately understand their patients' injuries and assisting them in efficiently making sound decisions to avoid diagnostic delays that can negatively impact postoperative outcomes.

Keywords Lisfranc injury, Myerson classification, Fracture line, 3D mapping

†Lei Zhang, Songtao Jiang and Ruihan Wang are the co-first authors.

*Correspondence:
Guoyou Wang
wangguoyou1981@swmu.edu.cn
[1]Department of Orthopedics, The Affiliated Traditional Chinese Medicine Hospital, Southwest Medical University, Luzhou, China
[2]Luzhou Key Laboratory of Orthopedic Disorders, Luzhou, China
[3]Institute of Integrated Chinese and Western Medicine, Southwest Medical University, Luzhou, China
[4]School of Clinical Medicine, Southwest Medical University, Luzhou, China
[5]School of Physical Education, Southwest Medical University, Luzhou, China
[6]Department of Rehabilitation, Yibin Integrated Traditional Chinese and Western Medicine Hospital, Yibin, China
[7]School of Traditional Chinese and Western Medicine, Southwest Medical University, Luzhou, China

Introduction

Lisfranc injuries are relatively uncommon, accounting for only 0.2% of all fractures [1, 2]. Lisfranc injuries have increased in recent years due to an increase in high-intensity athletic training, accounting for more than 15% of all athletic injuries [3–6]. In most cases, these injuries are high-energy trauma that results in fractures of the Lisfranc joint as well as soft-tissue injuries surrounding the joint [7, 8]. In addition, this injury is often accompanied by subluxation of the TMT joint as well as metatarsal or tarsal fractures and the first tarsometatarsal (TMT) joint injuries [9–11]. Because of its complex anatomy, diverse pathogenetic factors, and injury mechanisms, Lisfranc injuries often present in multiple forms. Assuming that a Lisfranc lesion goes undetected or is inappropriately treated. In that case, the progressive deformity may develop, posttraumatic osteoarthritis (OA), and instability, which can occur in up to half of the cases of Lisfranc fracture dislocations [12]. Given the unique bone structure and ligamentous complex of the Lisfranc articulation, Lisfranc injuries are more complex, which is currently an enormous problem in the diagnosis and treatment of surgical patients [13, 14]. However, reasonable classification pattern can provide surgeons with meticulous clinical decisions and surgical planning.

Existing major classifications of Lisfranc injuries to describe displacement are mainly the Quenu, Kuss, and Myerson classifications [15–17]. Among these, the Quenu and Kuss classifications cannot assess injury severity, nor can they determine reasonable treatment or assess prognosis [8]. In the current study, the Myerson classification focuses on the injury pattern of Lisfranc injuries (fracture dislocations) as well as partial injuries of Lisfranc joints, but still the fracture phenomenon in Lisfranc injuries has not been systematically analyzed. Because of its widespread application, this paper is thus based on the Myerson classification to investigate it.

Three-dimensional (3D) fracture maps and heat maps are new techniques to visualize fracture distribution information, allowing a clear view of the location and frequency of fracture line distribution [18, 19]. At present, with the recent widespread use of 3D Computed tomography (CT) technology, it offers great convenience in furthering our understanding of foot injury [20]. The distribution of fracture lines, fracture morphology, fracture mechanism, and fracture pattern in the foot can be further investigated. This technique has been used extensively for various fracture types, but fracture line-related studies of Lisfranc injuries have not been performed. Therefore, the primary purpose of this study was to investigate the fracture line distribution characteristics of Lisfranc injuries by heat map techniques applied to 3D CT imaging to demonstrate fracture morphology in different Myerson types comprehensively and to summarize the fracture probabilities for different kinds of cases. This study aims to better assist surgeons in communicating the extents of Lisfranc injuries and assist shell physicians in treating this complex injury by presenting thermal imaging and morphologic features of fracture lines.

Materials and methods

Study sample and specimen selection

The research complied with protocols approved by the Medical Ethics Review Board of Affiliated Traditional Chinese Medicine Hospital of Southwest Medical University (BY2022025). CT data for patients diagnosed with Lisfranc injury between 2018 and 2022, were retrospectively analyzed. Inclusion criteria: (i) Lisfranc injury; (ii) Significant fracture line; (iii) Patient age ≥ 18 years. Exclusion criteria: (i) previous history of Lisfranc joint deformity; (ii) pathological fracture; (iii) CT scans of quality not to meet 3D CT modeling needs. We extracted CT data from a healthy adult (height 172 cm, weight 60 kg, foot length 24 cm) and created a standard foot model. This standard foot model can represent a general population without foot injury and deformity.

Fracture and heat mapping

Fracture-related CT data was acquired using a 128-slice spiral computer graphics scanner (Siemens Somatom, Thüringen, Germany). Mimics 21.0 software (Materialise, Leuven, Belgium) was used to reconstruct 3D models based on DICOM(Digital Imaging and Communications in Medicine) scans from a healthy adult male. The whole foot model is retained as the standard model. DICOM data of 157 Lisfranc injuries presenting with fracture fracture lines were imported into Mimics 21.0 for 3D reconstruction and virtual repositioning of fracture fragments, exported in STL format. In order to align the reconstructed 3D fracture model to the standard foot model, the STL file was imported into the 3-Matic 13.0 (Materialise, Leuven, Belgium) software. Automated fitting was used for the alignment process, which was examined from the joint surface view. However, some unstable fracture regions still require manual segmentation and alignment. Bone fracture lines were represented using 3-Matic 13.0 boundary lines, and the boundary lines were projected onto the standard model. Various fracture lines were classified based on Myerson's classification and fracture line distribution characteristics. The fracture mapping graphs were saved in TXT format with coordinates accurate to 0.0001 mm, expressed in the (x, y, z) form. Fracture lines were converted into 3D heat maps with the help of the E-3D Digital Medical Platform (Central South University, Changsha, China) software. A heat map was altered based on the frequency of occurrence of fracture lines in the 3D model at each site. Considering

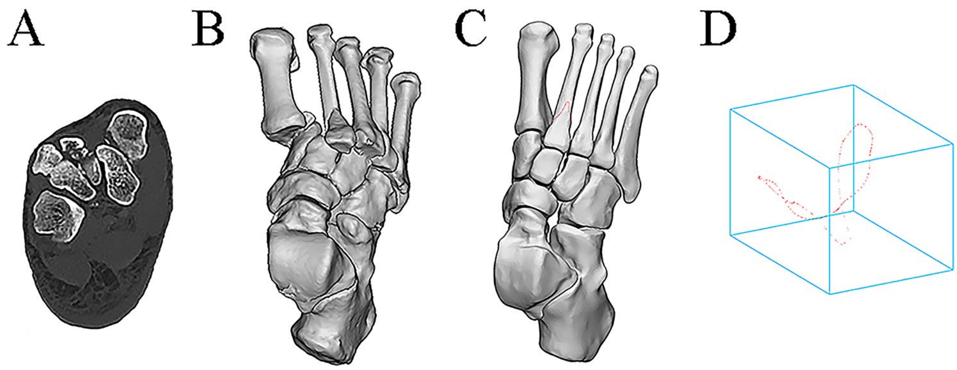

Fig. 1 Method used to map the fractures of the Lisfranc injury. (**A**) CT images of the Lisfranc damage. (**B**) Reconstruction of the injured foot and reduction of the fracture fragments in Mimics 21.0 software. (**C**) Fracture lines were paired and plotted in the 3-Matic 13.0 software. (**D**) Data sets from which the fracture lines were extracted

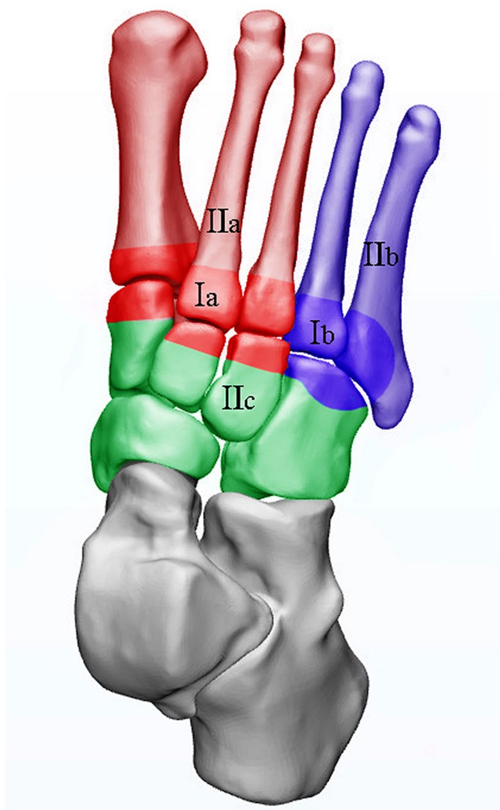

Fig. 2 On the bone surface, the different colored regions represent the different types

the possibility of a slight human error in drawing the fracture lines and morphological differences in the foot, we set the radiation distance for each line at 5 mm and employed distance weighting during the subsequent calculations (Fig. 1).

Novel Lisfranc fracture pattern

The summarized fracture lines were classified according to whether the fracture involved the TMT joint or not, and were also reclassified according to the distribution site and distribution density. Lisfranc injuries were categorized into five types, including those involving the TMT joint: type Ia: located in the TMT joint comprising the medial and intermediate columns; and type Ib: located in the TMT joint comprising the lateral column. Not involving the TMT joint: type IIa: located within the first, second, and third metatarsals (metatarsals forming the medial and intermediate columns); type IIb: located within the fourth and fifth metatarsals (metatarsals forming the lateral columns); and type IIc: other fractures that do not involve the TMT joint (excluding types IIa and IIb) (Fig. 2).

Data analysis

Data was analyzed by descriptive and percentage analysis. We calculated the number of bone fracture lines according to the Myerson classification and the rate of fracture lines at different locations. A qualitative description of the frequency of fracture lines under different sorts was obtained using color changes in the heat map. Color bars depict high, medium, and low frequencies in the heat map.

To enhance statistical robustness, chi-square tests were performed to compare the frequency distribution of fracture lines among Myerson subtypes. Inter-observer reliability of the novel classification system was evaluated using Cohen's kappa coefficient, calculated from independent assessments by two senior orthopedic surgeons.

Statistical analysis revealed significant differences in fracture line distribution between Myerson subtypes. For example, fractures involving the first metatarsal (M1) were significantly more frequent in Myerson Type B2 compared to Type C2 (χ^2=12.4, $p = 0.002$). The inter-observer agreement for the novel classification system was substantial ($\kappa = 0.82$, 95% CI 0.74–0.89).

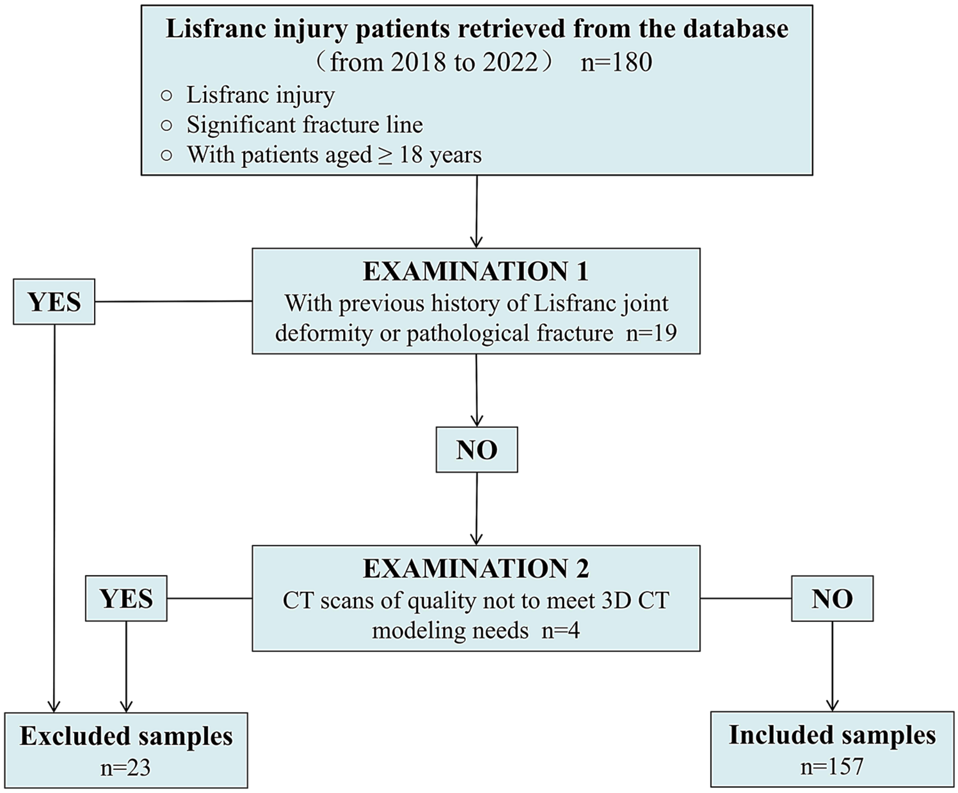

Fig. 3 The flowchart illustrates the inclusion and exclusion patient process

Table 1 Patient characteristics and Lisfranc injury characteristics

Character	Data ($n = 157$)
Female	63(40.1%)
Male	94(59.9%)
Age	45.52 ± 14.83
18-40y	49(31.2%)
41-70y	99(63.1%)
71-above	9(5.7%)

Table 2 Fracture line distribution characteristics. M1–M5: metatarsals 1–5; C1–C3: cuneiforms 1–3. Significant differences were observed between columns ($p < 0.05$)

Distribution site	Data ($n = 229$)
M1	92(40.17%)
M2	49(21.40%)
M3	25(10.92%)
M4	14(6.11%)
M5	18(7.86%)
C1	17(7.42%)
C2	8(3.49%)
C3	1(0.44%)
Cuboid bone	4(1.75%)
Navicular bone	1(0.44%)

Result

180 patients(from 2018 to 2022) with Lisfranc injuries and a clear fracture line were retrieved. Ultimately, 23 unsuitable data-sets were excluded, and 157 experimental data-sets were included (Fig. 3). The information of patients and the characteristics of Lisfranc injury characteristics were summarized (Table 1).

We used the Myerson classification to describe the types of fractures in our sample, and this classification was rated by a senior chief physician and an associate chief physician. Injury types were distributed as follows: Type A, $n = 26$(16.6%); Type B_1, $n = 32$(20.4%); Type B_2, $n = 61$(38.9%); Type C_1, $n = 20$(12.7%); Type C_2, $n = 18$(11.5%). As a final step, we gathered 229 fracture line groups and counted them according to the location of the fracture lines (Table 2).

3D mapping of Lisfranc injury lines

Whole view: The hot spots are centered in the proximal end of the first metatarsal and the second metatarsal, the medial cuneus bone as well as the first and second TMT joints.

View a: The hot spots are mainly concentrated on the proximal ends of the first and second metatarsals and are most dense where the two bones are adjacent to each other, with the fifth metatarsal joint as a subdense area and a small amount of distribution in the remaining bones.

View b: The hot spots are mainly concentrated on the proximal ends of the lateral first metatarsal and second metatarsal as well as the distal ends of the medial cuneiform and intermediate cuneiform, with the third and fifth metatarsals as subdense areas, and the rest of the bones distributed in small numbers.

View c: The hot spots are mainly concentrated on the entire first metatarsal joint as well as the top of the second metatarsal joint, and the rest of the bones are distributed in small numbers.

View d: The hot spots are mainly concentrated on the top of the medial cuneiform and intermediate cuneiform, and there are a few other portions, and the rest of the bones are distributed in small numbers (Fig. 4).

3D mapping of Myerson classification

Type A: The hot spots and fracture lines are mainly concentrated in the proximal part of the second metatarsal, with the fracture line wrapping around the second metatarsal in a ring-like fashion, the articular surface of the second metatarsal being the most severely involved, and the proximal part of the first metatarsal and the intermediate cuneiform bone in a small number of distributions.

Type B_1: The hot spots and fracture lines are mainly concentrated on the lateral aspect of the proximal end of the first metatarsal and also involve the first metatarsal stem, with the entire articular surface of the first metatarsal being most severely involved, and small amounts of the second, third, and fourth metatarsals distributed.

Type B_2: The hot spots and fracture lines are mainly centered on the proximal ends of the five metatarsals, in addition to involving the first and second metatarsal stems; all five TMT joints were involved, with the first metatarsal and the medial cuneiform being the most severe.

Type C_1: The fracture lines and hot spots are distributed around the TMT joint, with the bases of the first and fifth metatarsal crest being more densely apposed.

Type C_2: The fracture lines and hot spots are widely distributed over the metatarsals, cuneiform bones, and navicular bone (Fig. 5).

3D mapping of novel Lisfranc classification

Involving the articular surface

Type I_a: Fracture lines and hot spots are mainly concentrated on all of the articular surfaces of the first metatarsal, as well as on the top of the articular surfaces of the second metatarsal, the medial cuneiform, the intermediate cuneiform, and to a lesser extent on the lower end of the articular surfaces of the third metatarsal and the lateral cuneiform.

Type I_b: Fracture lines and hotspots are mainly distributed parallel to the middle of the articular surface of the fourth metatarsal, and perpendicular to the lateral aspect of the articular surface of the fifth metatarsal.

Not involving the articular surface

Type II_a: Fracture lines and hot spots are concentrated in the middle and proximal parts of the first and second metatarsal stems, as well as in the proximal part of the third metatarsal, with most of the fracture lines perpendicular to the long axis of the bone.

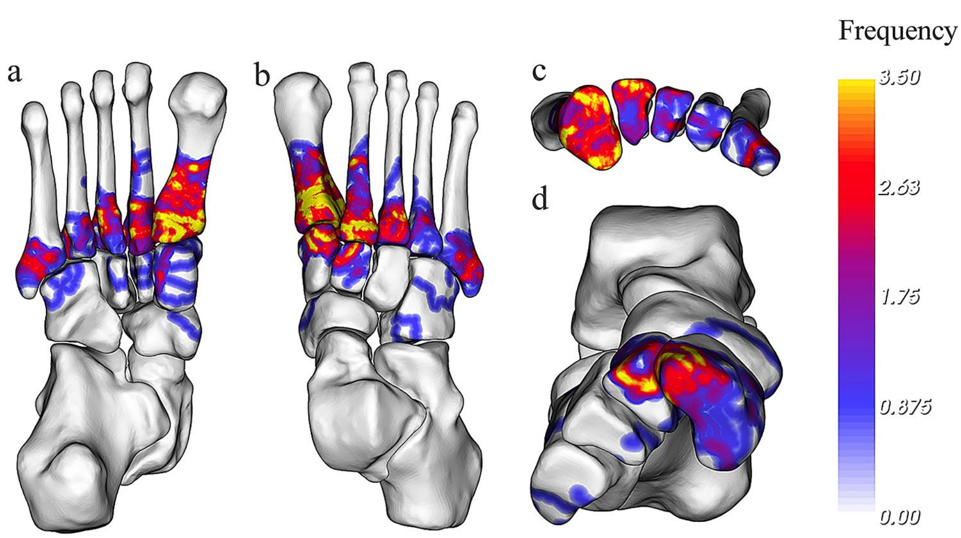

Fig. 4 Distribution and hotpots of fractures in Lisfranc injury (**a**: the bottom view; **b**: the top view; **c**: the back view of the TMT joint; **d**: the frontal view of the TMT joint). The proportion of the heat map represents the relative frequency of the brake lines. Color gradient indicates relative frequency of fracture lines, ranging from blue (lowest) to red (highest)

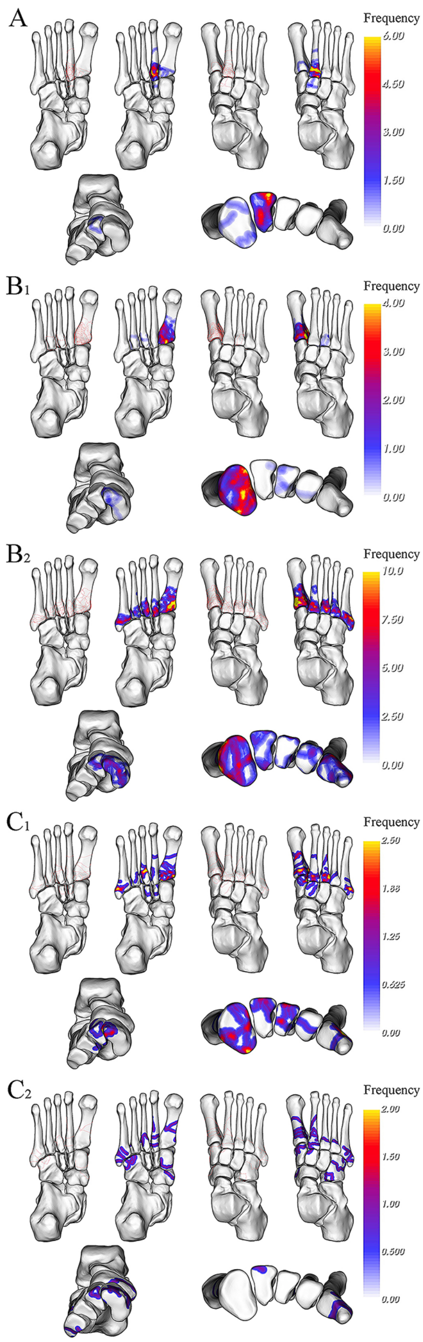

Fig. 5 Distribution and hotpots of fractures by Myerson classification. The scale of the heatmap represents the relative frequency of fracture lines. Color gradient indicates relative frequency of fracture lines, ranging from blue (lowest) to red (highest)

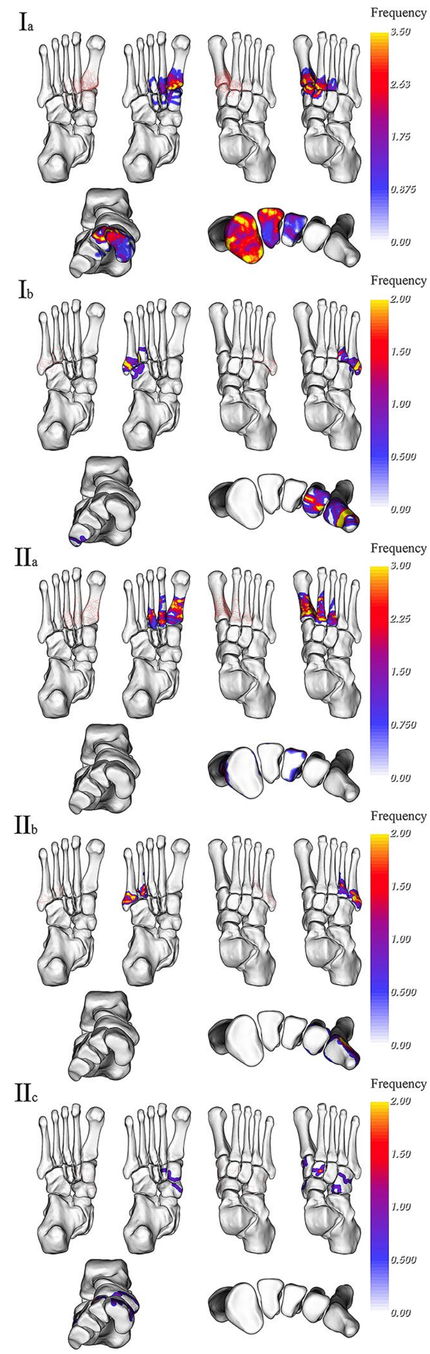

Fig. 6 Distribution and hotpots of fractures by new classification. The scale of the heatmap represents the relative frequency of fracture lines. Color gradient indicates relative frequency of fracture lines, ranging from blue (lowest) to red (highest)

Type $\mathrm{II_b}$: Fracture lines and hot spots are centered on the proximal end of the fourth metatarsal, and on the lateral side of the proximal end of the fifth metatarsal.

Type $\mathrm{II_c}$: The fracture lines and hot spots are an outer TMT fracture exclusive of Type $\mathrm{II_a}$ and Type $\mathrm{II_b}$ (Fig. 6).

Discussion

Lisfranc injury is named after 18th-century surgeon Jacques Lisfranc de St. Martin, who described this type of foot injury and significantly contributed to its treatment without precedent [21]. The Lisfranc joint is a group of joints located between the base of the metatarsus and the bones of the midfoot, and when this area is injured, it can result in dislocation or fracture of the joint and can be accompanied by damage to soft tissues (such as ligaments) [22]. It can lead to long-term pain and disability if left untreated or treated incorrectly [23]. Quenu and Kuss Classified this injury and summarized a set of classification methods for his displacement. It is based on the degree of destruction of the anterior and posterior part of the middle metatarsal joint and is divided into Type I, Type II, and Type III [16]. Meanwhile, the system also serves as the basis for several tracking classification schemes currently used in clinical practice [24]. Hardcastle et al. in 1982 modification of the typing: type A, in which all metatarsals are moved in one direction, is fully coherent; it is partially in conflict with the direction in which one or more metatarsals are displaced in type B; and type C, in which the removal of the fracture is entirely inconsistent. However, because of their limitations that do not contribute to management as well as to predict outcomes, such classification methods were soon replaced by other methods [8].

The Myerson system is an alternative classification system for lesions to the Lisfranc joint complex based on the bony anatomy and biomechanical properties of lesions to the Lisfranc joint complex [15, 17]. Myerson's typology is based on the skeletal anatomy and biomechanical features of lesions to the Lisfranc joint complex. Type A refers to the total incongruity of the tarsometatarsal joint; type B describes isolated incongruity patterns of the tarsometatarsal joint; type C is divergently displaced respectively. Due to the complexity of Lisfranc damage, Myerson subdivided previous type B and C types into B_1, B_2, C_1 and C_2. Compared to other classifications, Myerson typography more accurately characterizes injuries to the Lisfranc joint complex and may better guide surgical treatment. For this reason, the Myerson typeface is the most commonly used classification method and has become an integral part of modern foot and ankle surgery. Currently, there are multiple classifications of Lisfranc injury dislocations, particularly TMT dislocations, metatarsal displacement, and occult fractures. However, no study has yet summarized the fracture characteristics of Lisfranc injuries, such as the distribution of metatarsal and cuneiform fractures, and the extent of injury.

Myerson classification is one of the most widely used in the classification of Lisfranc injuries and is essential to differentiate between different degrees of Lisfranc injuries. On the other hand, in the Myerson classification, especially in the C_1 and C_2 subtypes, we can observe fracture lines dispersed in the midfoot in the fracture line drawing and thermogram. This suggests that the Myerson classification does not focus on the fracture characteristics of Lisfranc injuries and that its classification does not predict the site and extent of fractures, despite the addition of occult fractures in recent studies. Therefore, we propose a classification that effectively summarizes the fracture characteristics of Lisfranc injuries to further indicate the fracture characteristics of Lisfranc injuries as well as a diagnostic and treatment flowchart to help clinicians standardize management.

The fracture mechanism is mainly interpreted by morphological structure and rarely simulated by biomechanical tests. In morphological and structural studies, the second TMT joint is concave relative to the surrounding TMT joint, forming a tenon structure that further promotes bone stability, making this particular joint the "cornerstone" of the arch and the entire midfoot complex. At the same time, its unique structure also determines the high fracture rate of the joint [25, 26]. The complexity of Lisfranc injuries means that the pattern of injury is not simply one of displacement, but is often accompanied by fractures and ligamentous injuries.

Long-term functional outcomes of Lisfranc injuries remain a critical concern. Recent studies suggest that posttraumatic osteoarthritis (OA) develops in up to 40% of patients, particularly when articular congruity is not fully restored [27]. Our heat map analysis highlights the high fracture density in the medial cuneiform and second metatarsal base, regions biomechanically linked to midfoot stability. Future studies should correlate these fracture patterns with gait analysis or patient-reported outcomes (e.g., FAAM scores) to refine prognostic models.

Therefore, we can combine the single fracture line type of Lisfranc injury with the Myerson classification. Clinically, it is obvious that Lisfranc injuries often have multiple fracture lines due to their injuries, which can be supplemented by the combined fracture line types. The combinatorial pattern may have an important role in the graded assessment of Lisfranc injuries. However, simply combining the Myerson classification with a classification schema based on fracture lines can lead to confusion and hinder understanding. For this reason, we proposed the following classification scheme for Lisfranc injuries: step 1: assessment of whether ligamentous injuries are involved; step 2: assessment of Lisfranc injury pattern (Myerson classification); step 3: assessment of whether a fracture is present and assessment of the extent (Fig. 7). In this case, because of the complexity of the TMT joint, we only needed to analyze the spacing between C1-M2 and M1-M2 for initial assessment when performing Step 1 [28].

The characteristics of each type of fracture vary: type I_a fracture cracks are predominantly avulsion cracks with a low degree of displacement, a low number of comminuted cracks, and inevitably broken fragments; type I_b fractures are mainly oblique, with a high degree of displacement, especially in the fifth metatarsal, where the fracture fragments are often displaced laterally; type II_a

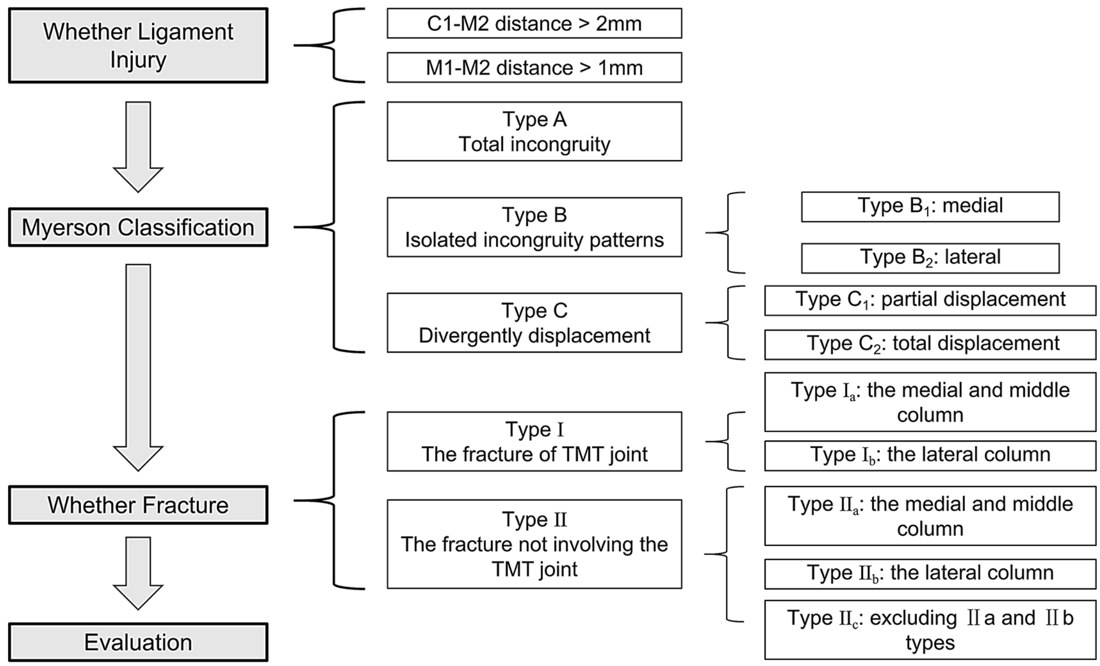

Fig. 7 Classification program for Lisfranc injuries. Step 1: Ligament injury assessment via C1-M2/M1-M2 spacing; Step 2: Myerson classification; Step 3: Fracture extent evaluation (novel classification)

fractures are mostly transversely oblique, with the first metatarsal displaced less than the second metatarsal on average, but the vast majority of the comminuted fractures involve the first metatarsal; type II_b fracture fractures are predominantly avulsion fractures with a lower degree of displacement; type II_c fractures are mostly incomplete fractures, but some fragments are present.

After CT scanning and 3D reconstruction, the specific type of injury is categorized according to the Myerson classification in order to help the clinician make an initial judgment based on the type of ligament injury and the type of fracture injury and to further determine whether to operate surgical access and surgical approach. Optimal prognosis in patients with Lisfranc injuries is critically dependent on anatomical joint repositioning combined with immobilization and selection of an appropriate surgical approach [29]. For example, type I_a, II_a, and some II_c fractures can be made with an incision in the intermetatarsal space between the M1 and M2, followed by reduction and screw fixation; type I_b, II_b, and others can be made with a longitudinal incision in the direction parallel to the fourth metatarsal, followed by reduction and K-wire resurfacing. In essence, this novel classification complements the fracture component of Lisfranc injuries through thermographic reclassification, which can effectively aid in the treatment and prognosis of the injury.

While our classification provides a spatial framework for fracture patterns, its clinical utility requires validation through prospective trials. We propose a multicenter study integrating the novel classification with standardized surgical protocols (e.g., open reduction vs. percutaneous fixation) and outcome metrics such as the AOFAS midfoot score and radiographic OA progression. Additionally, machine learning algorithms trained on 3D heat maps may enhance diagnostic accuracy and reduce inter-observer variability.

To validate the clinical utility of the novel classification system, we propose a prospective multicenter cohort study comparing it with the Myerson classification. The study will enroll 200 patients with acute Lisfranc injuries, randomized into two groups: one managed via the novel classification-based protocol (surgical approach selected by fracture patterns) and the other via traditional Myerson-based protocols. Primary outcomes will include diagnostic accuracy (sensitivity/specificity of detecting instability), functional recovery (AOFAS midfoot score at 12 months), and complication rates (e.g., posttraumatic OA). Secondary outcomes will assess intraoperative decision-making efficiency (time to final surgical plan). This design aligns with recent recommendations for validating orthopedic classifications (Table 3).

Conclusion

This study aimed to apply 3D mapping and thermography to characterize fracture patterns in Lisfranc injuries, to better help surgeons understand the extent of Lisfranc injuries, and to help surgeons treat this complex injury. In addition, a Lisfranc injury flowchart was developed that included Myerson classification, ligament injuries, and the degree of fracture injury. To further develop an

Table 3 Correlation between novel classification subtypes and AOFAS scores

Subtype	AOFAS Score (Mean ± SD)	*p*-value*
Ia	85 ± 8	0.03
Ib	78 ± 10	0.12
IIa	82 ± 9	0.08
IIb	88 ± 7	0.01
IIc	75 ± 11	0.21

*Compared to Myerson-based historical controls

assessment protocol for Lisfranc injuries that incorporates displacement and fracture, it is necessary to achieve a larger sample size of participants and to use statistics to devise a rating scale that evaluates the severity of Lisfranc injuries.

Limitations

Limitations of the present study include the following: first, the small number of patients in the sample did not allow for the use of statistics to devise a scale to rate the severity of Lisfranc injury; second, due to the large degree of anatomical variability in the foot, the fracture reconstruction models sometimes do not match the foot exactly and must be manually aligned and repositioned.

Acknowledgements
Not applicable.

Author contributions
LZ: conceptualization, software, methodology, funding acquisition. SJ: conceptualization, software, methodology, writing-original draft, validation. RW: writing-original draft, validation, investigation. XC: data curation, visualization. WW: data curation, supervision. GW: conceptualization, project administration, writing-review and editing.

Funding
The study received grants from Sichuan Science and Technology Program, project number:2022YFS0609. Scientific Research Cultivation Project of The Affiliated Traditional Chinese Medicine Hospital, Southwest Medical University, project number: 2022-CXTD-08. Integrated traditional Chinese and Western Medicine Special Project of Southwest Medical University (Optimizing Basic Disciplines Plan), project number: 2023ZYYJ03.

Data availability
No datasets were generated or analysed during the current study.

Declarations

Ethical approval
The research complied with protocols approved by the Medical Ethics Review Board of Affiliated Traditional Chinese Medicine Hospital of Southwest Medical University (BY2022025).

Consent to participate
Not applicable because of the retrospective design of the investigation.

Consent for publication
All individual data consent to publish.

Competing interests
The authors declare no competing interests.

Received: 7 January 2025 / Accepted: 27 February 2025

Published online: 12 March 2025

References

1. Desmond EA, Chou LB. Current concepts review: Lisfranc injuries. Foot Ankle Int. 2006;27(8):653–60. https://doi.org/10.1177/107110070602700819.
2. Garrick JG, Requa RK. The epidemiology of foot and ankle injuries in sports. Clin Sports Med. 1988;7(1):29–36.
3. DeOrio M, Erickson M, Usuelli FG, Easley M. Lisfranc injuries in sport. Foot Ankle Clin. 2009;14(2):169–86. https://doi.org/10.1016/j.fcl.2009.03.008.
4. Kalia V, Fishman EK, Carrino JA, Fayad LM. Epidemiology, imaging, and treatment of Lisfranc fracture-dislocations revisited. Skeletal Radiol. 2012;41(2):129–36. https://doi.org/10.1007/s00256-011-1131-5.
5. Meyer SA, Callaghan JJ, Albright JP, Crowley ET, Powell JW. Midfoot sprains in collegiate football players. Am J Sports Med. 1994;22(3):392–401. https://doi.org/10.1177/036354659402200316.
6. Ponkilainen V, Kuitunen I, Liukkonen R, Vaajala M, Reito A, Uimonen M. The incidence of musculoskeletal injuries: a systematic review and meta-analysis. Bone Joint Res. 2022;11(11):814–25. https://doi.org/10.1302/2046-3758.1111.BJR-2022-0181.R1.
7. Richter M, Wippermann B, Krettek C, Schratt HE, Hufner T, Therman H. Fractures and fracture dislocations of the midfoot: occurrence, causes and long-term results. Foot Ankle Int. 2001;22(5):392–8. https://doi.org/10.1177/107110070102200506.
8. Thompson MC, Mormino MA. Injury to the tarsometatarsal joint complex. J Am Acad Orthop Surg. 2003;11(4):260–7. https://doi.org/10.5435/00124635-200307000-00005.
9. Mulcahy H. Lisfranc injury: current concepts. Radiol Clin North Am. 2018;56(6):859–76. https://doi.org/10.1016/j.rcl.2018.06.003.
10. Wong LH, Chrea B, Atwater LC, Meeker JE. The first tarsometatarsal joint in Lisfranc injuries. Foot Ankle Int. 2022;43(10):1308–16. https://doi.org/10.1177/10711007221112090.
11. Wright MP, Michelson JD, Lisfranc injuries. BMJ. 2013;347:f4561. Published 2013 Jul 23. https://doi.org/10.1136/bmj.f4561
12. Stavlas P, Roberts CS, Xypnitos FN, Giannoudis PV. The role of reduction and internal fixation of Lisfranc fracture-dislocations: a systematic review of the literature. Int Orthop. 2010;34(8):1083–91. https://doi.org/10.1007/s00264-010-1101-x.
13. Moracia-Ochagavía I, Rodríguez-Merchán EC. Lisfranc fracture-dislocations: current management. EFORT Open Rev. 2019;4(7):430–44. https://doi.org/10.1302/2058-5241.4.180076. Published 2019 Jul 2.
14. Panchbhavi VK, Molina D 4th, Villarreal J, Curry MC, Andersen CR. Three-dimensional, digital, and gross anatomy of the Lisfranc ligament. Foot Ankle Int. 2013;34(6):876–80. https://doi.org/10.1177/1071100713477635.
15. Myerson MS, Fisher RT, Burgess AR, Kenzora JE. Fracture dislocations of the tarsometatarsal joints: end results correlated with pathology and treatment. Foot Ankle. 1986;6(5):225–42. https://doi.org/10.1177/107110078600600504.
16. Quenu E, Kuss G. Etude Sur les luxations du meta-tarse. Rev Chir Paris. 1909;39:281.
17. Sivakumar BS, An VVG, Oitment C, Myerson M. Subtle Lisfranc injuries: A topical review and modification of the classification system. Orthopedics. 2018;41(2):e168–75. https://doi.org/10.3928/01477447-20180213-07.
18. Cole PA, Mehrle RK, Bhandari M, Zlowodzki M. The Pilon map: fracture lines and comminution zones in OTA/AO type 43C3 Pilon fractures. J Orthop Trauma. 2013;27(7):e152–6. https://doi.org/10.1097/BOT.0b013e318288a7e9.
19. Yang Y, Yi M, Zou C, Yan ZK, Yan XA, Fang Y. Mapping of 238 quadrilateral plate fractures with three-dimensional computed tomography. Injury. 2018;49(7):1307–12. https://doi.org/10.1016/j.injury.2018.05.026.
20. Essa A, Levi A, Ron TG, Ner EB, Finestone AS, Tamir E. The role of three dimension computed tomography in Lisfranc injury diagnosis. Injury. 2022;53(10):3530–4. https://doi.org/10.1016/j.injury.2022.07.032.
21. Cassebaum WH. Lisfranc fracture-dislocations. Clin Orthop Relat Res. 1963;30:116–29.
22. Myerson MS, Cerrato R. Current management of tarsometatarsal injuries in the athlete. Instr Course Lect. 2009;58:583–94.
23. Hardcastle PH, Reschauer R, Kutscha-Lissberg E, Schoffmann W. Injuries to the tarsometatarsal joint. Incidence, classification and treatment. J Bone Joint Surg Br. 1982;64(3):349–56. https://doi.org/10.1302/0301-620X.64B3.7096403.
24. Siddiqui NA, Galizia MS, Almusa E, Omar IM. Evaluation of the tarsometatarsal joint using conventional radiography, CT, and MR imaging. Radiographics. 2014;34(2):514–31. https://doi.org/10.1148/rg.342125215.

25. Clare MP. Lisfranc injuries. Curr Rev Musculoskelet Med. 2017;10(1):81–5. https://doi.org/10.1007/s12178-017-9387-6.
26. Weatherford BM, Anderson JG, Bohay DR. Management of tarsometatarsal joint injuries. J Am Acad Orthop Surg. 2017;25(7):469–79. https://doi.org/10.5435/JAAOS-D-15-00556.
27. Moracia-Ochagavía I, Rodríguez-Merchán EC. Lisfranc fracture-dislocations: current management. EFORT Open Rev. 2019;4(7):430–44. https://doi.org/10.1302/2058-5241.4.180076.
28. Robertson GAJ, Ang KK, Maffulli N, Keenan G, Wood AM. Return to sport following Lisfranc injuries: A systematic review and meta-analysis. Foot Ankle Surg. 2019;25(5):654–64. https://doi.org/10.1016/j.fas.2018.07.008.
29. Ahluwalia R, Yip G, Richter M, Maffulli N. Surgical controversies and current concepts in Lisfranc injuries. Br Med Bull. 2022;144(1):57–75. https://doi.org/10.1093/bmb/ldac020.

Publisher's note